

Modelling and Visualizing the Cahn-Hilliard-Cook Equation

K.A. Hawick and D.P. Playne

Computer Science, Institute for Information and Mathematical Sciences,
Massey University, North Shore 102-904, Auckland, New Zealand

k.a.hawick@massey.ac.nz; daniel.playne@gmail.com

Tel: +64 9 414 0800 Fax: +64 9 441 8181

Abstract

The Cahn-Hilliard-Cook equation continues to be a useful model describing binary phase separation in systems such as alloys and other physical and chemical applications. We describe our investigation of this field equation and report on the various discretisation schemes we used to integrate the system in one-, two- and three-dimensions. We also discuss how the equation can be visualised effectively in these different dimensions and consider how these techniques can usefully be applied to other partial differential equations.

Keywords: alloy; pde; 3-D visualisation; interactive; phase separation.

1 Introduction

This paper describes an investigation of phase separation in a binary system. The Cahn-Hilliard-Cook (CHC) *equation* gives a reasonable representation of phase separation and decomposition in a binary system, providing one accepts that it cannot be applied successfully without resorting to numerical methods. The Cahn-Hilliard-Cook *theory* is essentially a mean field approximation to the time-dependent Ginzburg-Landau equation for the free energy of a binary system. The differential equation that describes the phase separation cannot be solved analytically, and requires further approximation. Alternatively it can be solved numerically for a particular set of parameters.

This paper extends work begun in 1988 and included in [1]. Recent work on faster general purpose computers has enabled greater exploration of the CHC parameter space and interactive visualisation of two- and three dimensional systems.

2 Cahn-Hilliard-Cook Equation

We consider a system of a mixture of two atomic species A and B, with some variable c_i that expresses which species is at a particular site i . Cahn-Hilliard-Cook (CHC) theory replaces these rapidly varying atomic concentration variables $\{c_i\}$ by a more smoothly varying continuous field variable $\phi(\mathbf{r})$ which represents an average value of the excess concentration of A-atoms over a macroscopic spatial cell. The field variable is a scalar defined to lie on $[-1, 1]$, with the extremum values representing an excess of B-atoms (-1) or an excess of A-atoms ($+1$).

The CHC field equation is derived using the Helmholtz free energy for an isotropic binary solid in solution and having a non-uniform composition. A convenient form for this is the Ginzburg-Landau functional [2]:

$$\frac{\mathcal{F}\{\phi(\mathbf{r})\}}{k_b T} = \frac{F_0}{k_b T} + \int_V \left\{ f\{\phi(\mathbf{r})\} - \frac{H}{k_b T} \phi(\mathbf{r}) + \frac{1}{2d} [R \nabla \phi(\mathbf{r})]^2 \right\} d\mathbf{r} \quad (1)$$

The scalar field $\phi(\mathbf{r})$ describes the composition as a function of position \mathbf{r} . The interaction range is described by $\frac{R}{d}$ and the applied field is H . For fixed atomic concentration, the applied field H can be set identically to zero for an equal concentration of A-type and B-type atoms.

The phase separating alloy may be thought of as a set of macroscopic cells, each containing a volume of space and a number of atomic sites. These cells must be large enough for a local instantaneous free energy function $f(\mathbf{r})$ to be defined, but small enough that the effect of ‘relevant’ short length scale composition fluctuations are not integrated out.

It is convenient to write this local free energy density function $f\{\phi(\mathbf{r}, t)\}$ in the Landau form:

$$f\{\phi(\mathbf{r}, t)\} = f_0 - \frac{1}{2}b(\phi(\mathbf{r}, t))^2 + \frac{1}{4}u(\phi(\mathbf{r}, t))^4 + \dots \quad (2)$$

where $b, u > 0$.

In a real material the number of atoms of a given species is conserved and hence the concentration field must also be. This is expressed by:

$$\frac{1}{V} \int_V \phi(\mathbf{r}, t) d\mathbf{r} = c_A \quad (3)$$

where V is the system volume, and c_A the concentration of atomic species A . This conservation law implies that the local concentration field obeys a continuity equation of the form:

$$\frac{d\phi(\mathbf{r}, t)}{dt} + \nabla \cdot \mathbf{j}(\mathbf{r}, t) = 0 \quad (4)$$

This defines a concentration current $\mathbf{j}(\mathbf{r}, t)$, assumed to be proportional to the gradient of the *local* chemical potential difference ¹ $\mu(\mathbf{r}, t)$ with constant of proportionality m , the mobility.

$$\mathbf{j}(\mathbf{r}, t) = -m\nabla\mu(\mathbf{r}, t) \quad (5)$$

The chemical potential difference is, by definition:

$$\mu(\mathbf{r}, t) = \frac{d\mathcal{F}\{\phi(\mathbf{r}, t)\}}{d\phi(\mathbf{r}, t)} \quad (6)$$

Where \mathcal{F} is the Landau functional given above in equation 1. Differentiating this functional with respect to ϕ and assuming a scalar mobility yields the chemical potential difference as:

$$\mu(\mathbf{r}, t) = \left. \frac{\partial f}{\partial \phi} \right|_T - \frac{R^2}{d} k_b T \nabla^2 \phi(\mathbf{r}, t) \quad (7)$$

which when substituted into the continuity equation 4 gives the Cahn-Hilliard equation [2] for the concentration field.

$$\frac{\partial \phi(\mathbf{r}, t)}{\partial t} = m \nabla^2 \left(\left. \frac{\partial f(\phi(\mathbf{r}, t))}{\partial \phi} \right|_T - K \nabla^2 \phi(\mathbf{r}, t) \right) \quad (8)$$

Where the parameter K is defined as:

$$K = \frac{R^2}{d} k_b T \quad (9)$$

Expanding equation 8 we obtain:

$$\frac{\partial \phi}{\partial t} = m \nabla^2 (-b\phi + u\phi^3 - K \nabla^2 \phi) \quad (10)$$

It is usual to truncate the series in the free energy at the ϕ^4 term, although some work has used up to the ϕ^6 term [3].

¹The global chemical potential is identified with the field term in the Ising Hamiltonian and is identically zero for a system of conserved concentration

2.1 Cahn-Hilliard Theory

Equation 8 is non-linear and therefore cannot be solved analytically, although a numerical approach is possible. As described in [2], the Cahn-Hilliard theory proceeds by linearising the equation around $\phi = c_A$ to obtain:

$$\frac{\partial(\phi - c_A)}{\partial t} = m \nabla^2 \left(\left. \frac{\partial f}{\partial \phi} \right|_{T, c_A} - K \nabla^2 (\phi - c_A) \right) \quad (11)$$

This is Fourier-transformed using:

$$\Phi(\mathbf{q}, t) = \int e^{i\mathbf{q} \cdot \mathbf{r}} (\phi(\mathbf{r}, t) - c_A) d\mathbf{r} \quad (12)$$

to yield:

$$\Phi(\mathbf{q}, t) = \Phi(\mathbf{q}, t=0) e^{B(\mathbf{q})t} \quad (13)$$

and the time amplification factor B is given by:

$$B(\mathbf{q}) = -m \mathbf{q}^2 \left(\left. \frac{\partial f}{\partial \phi} \right|_{T, c_A} + K \mathbf{q}^2 \right) \quad (14)$$

The structure function can be then obtained as an auto-correlation of the concentration field:

$$S(\mathbf{q}, t) = \langle \Phi(-\mathbf{q}, t) \Phi(\mathbf{q}, t) \rangle|_T \quad (15)$$

Re-writing this in terms of the values just prior to the quench gives:

$$S(\mathbf{q}, t) = \langle \Phi(-\mathbf{q}, t=0) \Phi(\mathbf{q}, t=0) \rangle|_T e^{2B(\mathbf{q})t} \quad (16)$$

The prefactor in 16 is the static structure factor of the initial state at T_0 , just prior to the quench.

$$S_0(\mathbf{q}) = \langle \Phi(-\mathbf{q}, t=0) \Phi(\mathbf{q}, t=0) \rangle|_{T=T_0} \quad (17)$$

It is evident then that the linearised Cahn-Hilliard theory implies that fluctuations of \mathbf{q} present in the initial state will grow exponentially with time following the quench if $B(\mathbf{q}) > 0$ but will decay to zero for $B(\mathbf{q}) < 0$. There is an implied critical wavevector \mathbf{q}_c for which $B(\mathbf{q}) \equiv 0$. There has been some controversy in the literature [4] about the validity of this linearised theory, but it seems clear that the theory is not valid for systems with short range interactions such as the alloy model used in this work. A full discussion of the failings of the theory is left to [4].

2.2 Cook's Extension to Cahn-Hilliard

The Cahn-Hilliard theory as described above is essentially a mean field theory. It approximates the interactions between the concentration variables by a mean value and ignores thermal fluctuations. It might be expected that consequently it will incorrectly predict the dynamic behaviour of

the system. A simple extension to equation 8 was considered by Cook [5] in which an additional random force term ζ is added to give:

$$\frac{\partial \phi(\mathbf{r}, t)}{\partial t} = m \nabla^2 \left(\frac{\partial f(\phi(\mathbf{r}, t))}{\partial \phi} \Big|_T - K \nabla^2 \phi(\mathbf{r}, t) \right) + \zeta(\mathbf{r}, t) \quad (18)$$

This noise term is assumed to come from the very short time scale phonon modes of the alloy and is required to have the following properties:

$$\langle \zeta(\mathbf{r}, t) \rangle = 0 \quad (19)$$

$$\langle \zeta(\mathbf{r}, t) \zeta(\mathbf{r}', t') \rangle = -2k_b T m \nabla^2 \delta(\mathbf{r} - \mathbf{r}') \delta(t - t') \quad (20)$$

Equations 19 and 20 express two things. There is no overall drift force and the noise is uncorrelated in time, but partially correlated in space such that there are no long wavelength components in the noise spectrum. The magnitude of the noise is set by $k_b T$ and mobility m . More specifically, the ∇^2 in equation 20 expresses the conservation law for the field. A random force component which ‘piles up’ matter at one site must be exactly balanced by force contributions at neighbouring sites which deplete those sites of matter. The form of equation 20 ensures this is so.

The Cook noise term does not rescue the linearised theory from invalidity, but it does have important implications for numerical work. To date there have been no attempts to numerically solve equation 18, and is it still controversial whether the Cook noise term plays an important role in the long time dynamics of the alloy [6].

3 Numerical Solutions

Although equations 8 and 18 are highly non-linear in nature, it is nevertheless possible to numerically integrate them in time to follow the structure evolution. Two numerical methods suggest themselves for equations of this type, namely the well known finite differencing method and a lesser known spectral method such as the Fourier analysis and cyclic reduction algorithm (FACR) [7]. The former is relatively easy to set up and has been considered by other authors for very simple cases [6, 8]. Unfortunately it is fairly demanding of computational power to perform the time and spatial integrals of realistic systems. The FACR algorithm is more complicated to implement and while in general a spectral method is more suited to a studying a theory formulated in terms of waves in Fourier space, this algorithm is not suitable for comparison with the Monte

Carlo simulations in position space since it does not yield a real space representation of the concentration field.

3.1 Finite differencing Schemes

Consider equation 18 that we wish to integrate numerically: This can be re-cast as:

$$\frac{\partial \phi(\mathbf{r}, t)}{\partial t} = P(\mathbf{r}) \quad (21)$$

All the spatial dependence is now contained in the functional P , which can be discretised using a centred space representation. The scheme is illustrated below, initially only for a one dimensional system.

$$\begin{aligned} P_j^{(n)} = & \frac{M}{\Delta x^2} (-b\phi_{j-1}^{(n)} + 2b\phi_j^{(n)} - b\phi_{j+1}^{(n)} \\ & + u\phi_{j-1}^{(n)3} - 2u\phi_j^{(n)3} + u\phi_{j+1}^{(n)3} \\ & + \frac{1}{\Delta x^2} [-K\phi_{j-2}^{(n)} + 4K\phi_{j-1}^{(n)} - 6K\phi_j^{(n)} \\ & + 4K\phi_{j+1}^{(n)} - K\phi_{j+2}^{(n)}]) \\ & + \zeta_j^{(n)} \end{aligned} \quad (22)$$

where the spatial mesh of N points is indexed by $1 < j < N$, and the time discretisation mesh is indicated by $0 < n < \infty$. This centred space finite difference scheme is second order accurate in the spatial mesh size Δx and is optimal for a diffusion equation like the Cahn-Hilliard equation. Higher order accuracy in space is likely to be inherently unstable, and lower order is too limiting in terms of numerical accuracy [9]. This scheme was indeed found to be the best and can readily be extended to two and three dimensions.

It now remains to choose a discretisation scheme for the time domain. This is considerably more difficult. The obvious choice is the Forward-Time or Euler scheme and is only first order accurate in time. It is easily implemented as:

$$\phi_j^{(n+1)} = \phi_j^{(n)} + P_j^{(n)} \Delta t \quad (23)$$

In this scheme, each new grid point value of ϕ depends only on the previous generation of values. This method requires a small time-step but was only found to be sufficiently stable for the one dimensional system. A better scheme is required for higher dimensions. There are a number of widely used reliable schemes available [9], but the computational demands of such schemes prohibit their use, particularly in the present case where the computer technology is already being stretched to its limits in terms of speed.

The problem with the forward differencing scheme described above can be identified with the non-symmetric way it uses available data to perform each time step. Three

methods considered here for evaluating the ∇^2 operator in the Cahn-Hilliard equation. The $\nabla^2 \cdot \nabla^2 = \nabla^4$ contributes no new problem, it merely compounds the old one.

The staggered-leapfrog scheme is a well known method that is second order in time. It requires information from the two previous time steps to compute the next value and can be written as:

$$\phi_j^{(n+1)} = \phi_j^{(n-1)} + P_j^n \cdot \Delta t \quad (24)$$

This additional storage requirement is a disadvantage over the simpler forward differencing scheme, particularly for the large grids required. The staggered-leapfrog is surprisingly no improvement and indeed is considerably less stable for certain values of K , u , b and M . This anomaly can be understood by considering the effect of the alternating mesh used by this scheme. The two alternating meshes are in fact decoupled, so that drift instabilities can arise between the two meshes. This leads to rapid divergence of the field in opposing directions for each mesh.

This decoupling problem can be partially alleviated using the Lax scheme, whereby grid points used in the time-step calculation are replaced by interpolated values at half grid points $\phi_{j+\frac{1}{2}}^n$. This method uses a small *numerical viscosity* term obtained by adding a small fraction f of the value on the alternate grid to the grid calculation. This is somewhat unphysical and furthermore tends to damp out high frequency components in the evolving field. For this reason a better scheme is the two-step Lax-Wendroff method. In this scheme, the first operation is to evaluate the interpolated half-step points in time *and* space according to the Lax scheme, and then to use these intermediate values (which are discarded afterwards) to make a single time step movement.

$$\begin{aligned} \phi_{j+\frac{1}{2}}^{(n+\frac{1}{2})} &= \frac{1}{2} (\phi_{j+1}^{(n)} + \phi_j^{(n)}) + \frac{\Delta t}{2 \times 2} (P_{j+1}^{(n)} + P_j^{(n)}) \\ \phi_j^{(n+1)} &= \phi_j^{(n)} + \frac{\Delta t}{2} (P_{j-\frac{1}{2}}^{(n+\frac{1}{2})} + P_{j+\frac{1}{2}}^{(n+\frac{1}{2})}) \end{aligned} \quad (25)$$

This is a good *explicit* scheme found. It allows quite large time steps, and therefore relatively fast computation times for a given evolution time and very low mesh drifting despite low numerical viscosity.

The well known Runge-Kutta numerical integration method is more cumbersome to implement but we have experimented with both second order (also known as the mid-point method) and the fourth order scheme. Both perform well and on 21st century computer systems where we can afford the extra working storage

The schemes are summarised in table 1, they are described in [9, 10]. The upper limits on stability are determined from

the highest value of Δt that will converge for all reasonable parameter values *and* gives the *same* results with a 10% variation in Δt . The lower limit of stability is quoted as 0.00001, this resulting from the 32-bit real number precision employed in the calculations. This can be reduced at the expense of computational time, by resorting to 64-bit arithmetic.

3.2 Meaning of the CHC parameters

The Cahn-Hilliard-Cook equation is derived with parameters that are not obviously related to experimentally measurable properties of an alloy. The parameters u , b , m , and K that appear in equation 10 *can* be related to the microscopic parameters in the lattice gas model, by a comparison with mean field theory.

The mobility m appears only as a multiplicative constant and effectively controls the time scale. In numerical work it can be absorbed into the time-step of integration. The parameter $K = \frac{R^2}{d} k_b T$ reduces to $K = \frac{k_b T}{d}$ for the nearest neighbour interaction model, since:

$$R^2 = \frac{\sum_{i,j} (r_i - r_j)^2 (V_{i,j}^{A-A} + V_{i,j}^{B-B} - 2V_{i,j}^{A-B})}{\sum_{i,j} (V_{i,j}^{A-A} + V_{i,j}^{B-B} - 2V_{i,j}^{A-B})} \quad (26)$$

where the $V_{i,j}^{c_i-c_j}$ are the Ising coupling parameters and d is the spatial dimension.

This means K , like u and b have units of free energy density, and all contain a factor of $k_b T$ which can also be absorbed into the mobility or time scale. Standard mean field theory for the Ising model [11] shows that the parameter b controls the quench temperature for the model through the relation $b = \frac{T}{T_c^{MF}} - 1$, where T_c^{MF} is the mean field critical temperature discussed in chapter 2. This leaves the parameter u undetermined, but for numerical work it is convenient to set it to unity and employ the ratio $\frac{b}{u}$ to determine the interaction strength J^{A-A} . The combination of parameters $b = u = M = K = 1$, then corresponds to an infinite quench for an unknown linear time scale.

Increasing K corresponds to increasing the range of the model interactions, while changing the sign of K changes the ground state of the model to that of an ordered system, the exact nature of which will depend on the global concentration of A-atoms [3]. This present work considers only positive values of K .

Specific values of the Cook noise term appear less important than the fact of its mere presence. The correct magnitude is set by equation 20 and a convenient form is that of a Gaussian distribution centred on zero with $\sigma^2 = 2k_b T m$ in the units of the simulation, and with the properties dictated by equations 19 and 20.

Scheme	Range of Stability in Δt	Storage Requirements	Efficiency	Comment
FTCS (Euler)	0.01 – 0.00001	Low	Poor	Physical but inaccurate
Staggered-leapfrog	0.001 – 0.00001	Medium	Medium	Unreliable
Lax	0.05 – 0.00001	Medium	Good	Unphysical viscosity
Lax-Wendroff	0.1 – 0.00001	High	Very Good	Physical and reliable
Runge-Kutta 4	0.2 – 0.00001	Medium	Very Good	Physical and very reliable

Table 1: Finite Difference Schemes as applied to the Cahn-Hilliard-Cook Equation. Note that computational efficiency also takes account of how high the time step may be, since it is possible to integrate to longer simulated times much faster with an algorithm which allows large time steps.

4 One-Dimensional System

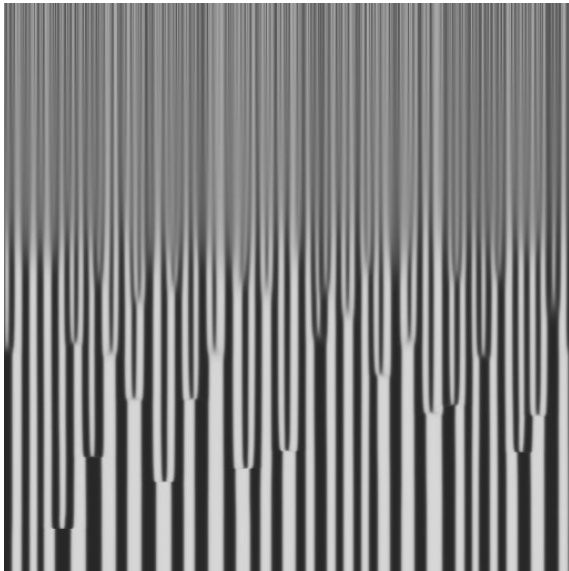


Figure 1: 1-D CHC system with space horizontally, and time downwards, plotted in \log_2 time, with each time row at times 0, 1, 2, 4, 8, 16, ...

A natural place to begin investigations is a symmetric quench from a temperature T_0 well above the two-phase coexistence curve to one below it T_1 . A completely random starting configuration is a good approximation to the case $T_0 \rightarrow \infty$.

A simple illustration of the important properties of the Cahn-Hilliard-Cook equation can be drawn from experiments with a one dimensional simulation. A one dimen-

sional system of 4096 sites was initialised randomly with $\phi_j \in [-0.25, 0.25]$, $\sum_j \phi_j = 0$, and numerically integrated with the parameter values $K = m = b = u = 1$ using a spatial mesh of $\Delta x = 1$ and a time step of $\Delta t = 0.01$ with the Forward-Time Centred Space (FTCS) scheme. The initially homogeneous mix separates out into two well defined phases. The real space evolution can be represented as an intensity plot for the composition field ϕ as a function of time vertically and space horizontally. The initial grey mix separated into a spatially modulated two phase structure. This can also be tracked for a longer time by examining the composition population.

It appears that for a pseudo-infinite quench, growth occurs, but slowly. The Cook noise term is zero for a quench to zero temperatures. At a temperature of $\frac{T_c}{4}$, the Cook noise term accelerates the initial growth process substantially. At a higher still temperature of $\frac{T_c}{2}$, there is sufficient thermal energy in the model system that the Cook term appears to have a less dramatic effect, although it still accelerates growth.

Figure 1 shows the formation of like domains of cells and the merging of domains over time. Time is plotted on a \log_2 scale to emphasise all timescales of the process. The resulting tree diagram shows how domains merge and as discussed in section 7 the number of separate domains N_D can be approximated by a power law in time t .

5 Two-Dimensional System

In two-dimensions the cells are able to interact in a different way from the simple left/right nearest neighbour interactions in a 1-D system. Figure 2 shows the time evolution

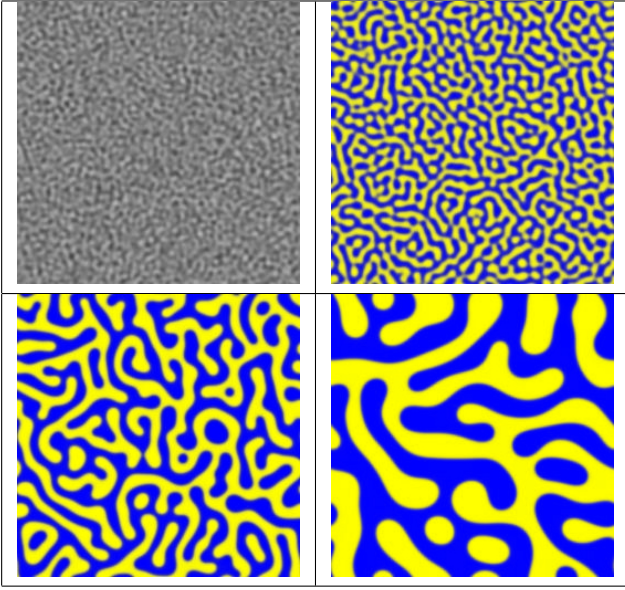


Figure 2: 2-Dimensional CHC simulation at $t = 0$ (top left), $t = 100$ (top right), $t = 1000$ (lower left) and $t = 10000$ (lower right)

of the composition population in a two-dimensional system. The random initial configuration forms domains which then coarsen and grow to form striated interleaving structures. Surface tension gradually draws these into just two separated domains, providing there is sufficient thermal energy in the system.

6 Three-Dimensional System

It is more difficult to track a three-dimensional system visually and more reliance must be placed on the size characterisation of the separating phases by averaged Fourier transforms. The peaks vary considerably in magnitude, but the peak positions can be well determined, and mapped to characteristic sizes.

The technology of visualisation in one- and two-dimensions has been well developed, however visualising the three-dimensional simulation is significantly more challenging. In this research the JOGL API [12] to the OpenGL library is used to render the three-dimensional simulation as a cube of cells. Each cell is rendered as a sphere and coloured relative to its atomic concentration value. The colour and opacity of each sphere $C_{x,y,z}$ is calculated according to the cell value $\sigma_{x,y,z}$ defined by equation 27.

A mixture of transparency combinations was explored and the combination of having one domain as mostly trans-

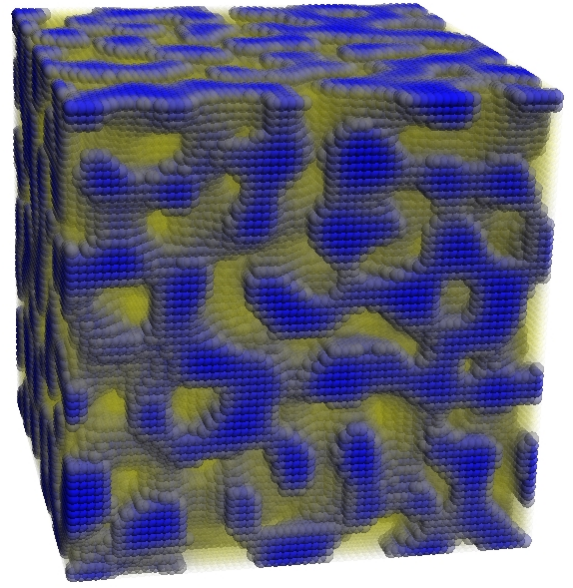


Figure 3: 3-D configuration with $64 \times 64 \times 64$ cells.

parent and the other relatively opaque allows the domain growth inside the cube to be seen the most clearly. One domain is seen as a complicated 3-D shape and the other as a cloud surrounding the shape. Navigating around the cube in 3-D allows the domains to be seen for the entire simulation.

7 Domain Growth

A number of macroscopic properties of the CHC system can be measured to characterise system bulk behaviour. Domains can be counted using a graph labelling technique and averaging over multiple sample random starting conditions and different temporal trajectories we can obtain a meaningful fit to the number of domains $N_D(t)$ as it varies with time. Figure 4 shows the number of distinct domains in different dimensional systems plotted against time. As can be seen from the log-log plots the system is quite well approximated by a power law in time $N_D \approx t^x$, where $d \equiv 2$ is the critical dimension.

8 Discussion and Conclusions

We have presented results from some numerical experiments on the Cahn-Hilliard -Cook equation and discussed the relative merits of different integration algorithms. While it is possible to use an adaptive step size method for time integration we find the fixed step size fourth-

$$C_{(x,y,z)} = \begin{cases} \text{rgb}(0.5 - 0.5\sigma_{x,y,z}, 0.5 - 0.5\sigma_{x,y,z}, 0.5 + 0.5\sigma_{x,y,z}, 0.5), & \text{if } \sigma_{x,y,z} > 0.0 \\ \text{rgb}(0.5 + 0.5\sigma_{x,y,z}, 0.5 + 0.5\sigma_{x,y,z}, 0.5 - 0.5\sigma_{x,y,z}, 0.05), & \text{if } \sigma_{x,y,z} \leq 0.0 \end{cases} \quad (27)$$

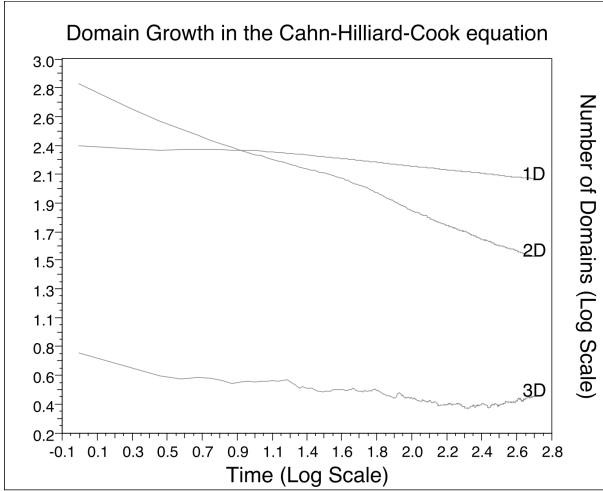


Figure 4: Domain growth plotted with time on a log-log scale, for systems of size 2048 cells; 256×256 cells; and $16 \times 16 \times 16$ cells respectively. Averages are over 10 separate configurations.

order Runge-Kutta algorithm entirely adequate and indeed more useful for studying regular time spaced samples.

Graphics libraries such as JOGL provide a manageable interface to an interactive simulation system and we have been able to study interactively the early stages of the three dimensional system for relatively interesting mesh resolutions.

Other equations such as the Time-dependent Ginzburg Landau equation employ a complex field variable and we are presently experimenting with graphical techniques to display such a field using partially opaque coloured values and rendered arrows to show phase.

References

- [1] Hawick, K.A.: Domain Growth in Alloys. Edinburgh University, Ph.D. Thesis (1991)
- [2] Cahn, J., Hilliard, J.: Free energy of a non-uniform system III. Nucleation in a two point compressible fluid. *J.Chem.Phys.* **31** (1959) 688–699
- [3] Tuszynski, J., Skierski, M., Grundland, A.: Short-range induced critical phenomena in the Landau-Ginzburg model. *Can.J.Phys.* **68** (1990) 751–755
- [4] Binder, K.: Mechanisms for the decay of unstable and metastable phases: Spinodal decomposition, nucleation and late-stage coarsening. In Stocks, G.M., Gonis, A., eds.: *Alloy Phase Stability*, Kluwer Academic (1989) 233–262
- [5] Cook, H.: Brownian Motion in Spinodal Decomposition. *Acta.Met* **18** (1970) 297–306
- [6] Toral, R., Chakrabarti, A., Gunton, J.D.: Numerical study of the Cahn-Hilliard equation in three dimensions. *Phys. Rev. Lett.* **60** (1988) 2311–2314
- [7] Buzbee, B., Golub, G., Nielson, C.: On Direct methods for solving Poisson's equation. *SIAM J.Num.Analysis* **7** (1970) 627–656
- [8] Milchev, A., Heermann, D.W., Binder, K.: Monte-carlo simulation of the Cahn-Hilliard model of spinodal decomposition. *Acta. Metall.* **36** (1988) 377–383
- [9] Press, W., Flannery, B., Teukolsky, S., Vetterling, W.: 17. In: *Numerical Recipes in C*. Cambridge University Press (1988) 636–688 Partial Differential Equations.
- [10] Allen, M., Tildesley, D.: *Computer simulation of liquids*. Clarendon Press (1987)
- [11] Binder, K.: *Theory of First Order Phase Transitions*. Mainz Preprint (1988)
- [12] Bryson, T., Russell, K.: *Java Binding for OpenGL (JOGL)* (2007)